7th International Energy Conversion Engineering Conference
2 - 5 August 2009, Denver, Colorado

AIAA 2009-4530

Theoretical and Experimental Study of Remote Sensing for Measuring Transport Emissions

Alon Davidy*[*]
Israel Military Industries (IMI), Ramat Hasharon, Israel, 47100

Yoram. Zvirin†& Leonid Tartakovsky[†]
Faculty of Mechanical Engineering, Technion - Israel Institute of Technology, Haifa, Israel, 32000

The problem of air pollution by motor vehicles is becoming more severe in the world. The standard methods for measuring the concentrations of pollutants emitted by vehicles may be performed only for very limited vehicle samples because of their cost and complexity. A novel method of "Remote Sensing" (RS) is developed to enable measurements of pollutants emitted by passing vehicles. The results of RS experiments, carried out in Israel and in the world, show that 10% of the gasoline vehicles fleet are responsible for about half of the total emissions. These results indicate that identifying these big polluters and repairing them could lead to significant improvement of the air quality. The remote sensing method for measuring pollutants concentrations is based on the attenuation of electromagnetic (or laser) beams, which are radiated from a source, traverse through the exhaust gas plume and detected by a sensor. Infra – Red (IR) and Ultra – Violet (UV) radiation absorption is applied to monitor the NO, HC, CO and CO_2 concentrations. The RS measurement is still in the development stage, and not yet accurate and reliable enough. Thus it cannot be used now to determine emission standards or to enforce them. The main objective of this work was to develop a theoretical model for the interpretation of RS measurements of gaseous pollutants and Particulate Matter (PM) emissions. A new method was developed for calculating the Optical Thickness (OT) of participating media containing exhaust gas mixture with scattering particles. The medium considered here is anisotropic and has wavelength dependent properties. The radiation absorption and scattering efficiencies of the particles were calculated according to Mie or Rayleigh theories and the gaseous absorption coefficients by the Line-By-Line (LBL) method. It is assumed that the concentration of each component in the plume can be calculated according to Gaussian dispersion model. A new analytical solution for the General Dynamic Equation (GDE) is employed in this algorithm. RS experiments were carried out, where emissions of about 14,000 vehicles were monitored and analyzed. The calculated results for the OT were fitted to the RS measurement results in order to obtain the gaseous pollutants concentrations and particles emission rates in the tailpipe outlet. Numerical results (for OT) compare favorably with experimental data. This model may be applied in current RS technologies as a supplement tool for monitoring PM.

Nomenclature

b = parameter in Gamma distribution , $1/m$.

c = speed of light, m/sec .

*[*] Researcher, IMI, Ramat-Hasharon, 47100/66, Israel.
† Professor, Head of Internal Combustion Engines Laboratory, Faculty of Mechanical Engineering, Technion, Israel Institute of Technology, Haifa, 32000, Israel.
[†] Doctor, Chief Engineer of Internal Combustion Engines Laboratory, Faculty of Mechanical Engineering, Technion, Israel Institute of Technology, Haifa, 32000, Israel.

d = particle diameter, m.

D^p = diffusion coefficient of particles, m^2/sec.

$D(\nu, \nu_i)$ = lorentizian probabilty of radiation absorption at wave number ν, m.

$f_1(n, \kappa)$ = function of particle radiative properties, dimmensionless.

$G(\nu_i)$ = gaussian probability of an absorber having a line in the interval $(\nu_i, \nu_i + d\nu_i)$, due to its thermal motion, m.

g = gravitation acceleration, m/sec^2

G_f = fuel consumption of the vehicle, kg/km.

h = planck constant, $J \cdot sec$.

k_a = absorption coefficient of the mixture composed of particles and gas, $1/m$.

$k_{a,j}$ = absorption coefficient of the j component, $1/m$.

k_B = boltzmann constant, J/kg.

k_s = scattering coefficient of the mixture composed of particles and gas, $1/m$.

L = the distance between the plume axis and RS transmitter, m.

L_1 = the distance between the plume axis and RS detector, m.

M = distribution in space of particles concentration, $1/m^3$.

M_g = molecular weight of exhaust gas, $kg/kmol$.

M_i = molecular mass of i component in the mixture, $kg/kmole$.

N = particles size distribution function with volume, $1/m^6$.

n = refractive index, relative refractive index, n_1/n_2, dimmensionless.

Na = avogadro number, dimmensionless.

N_g = number of gas components, dimmensionless.

p = pressure, kPa

Q = particle efficency, dimmensionless.

$Q(T)$ = partition function, of the absorbing molecule, dimmensionless.

Q_i = volumetric flow rate of component i emitted per unit time, m^3/sec.

Q_p = particle emission rate, $1/sec$.

$\overline{R}$ = universal gas constant, $kJ/kmol\,K$.

r = particle radius, m.

r_p = plume radius, m.

T = temperature, K.

t = time, sec.

T_s =standard temperature, K.

S_i' =intensity of line i, m.

U_v =vehicle mean velocity, m/sec.

x, y, z =cartesian coordinates, m.

z_A, z_B, z_C, z_D, z_E = parameters, dimmensionless.

Greek Symbols

η = combustion equation parameter.

κ = extinction coefficient, relative extinction coefficient κ_1/n_2 , dimmensionless.

Λ = air to fuel ratio, dimensionless.

λ = wave length, m.

μ_g = viscosity of exhaust gas, $kg/m\sec$.

ν_g = kinematic viscosity of exhaust gas, $m^2/\sec$.

ν_i = wave number of line i, $1/m$.

ξ = particle size parmeter, dimmensionless.

ρ_g = exhaust Gas density, kg/m^3.

ρ_p = particle density, kg/m^3.

σ_a = particle absorption cross section, m².

σ_s = particle scattering cross section, m².

σ_y, σ_z =standard deviations in y and z directions, m.

υ = particle volume, m^3

χ_i =mole fraction of component i in the plume, dimensionless.

Subscripts

a = absorbed

s = scattered

t =extincted

1 =Particle material

2 = medium

Superscripts

IR =infra red

UV =ultra violet

I. Introduction

MANY, indeed most, of our everyday methods of measurement are indirect. Objects are weigthed by observing how much they stretch a spring, temperature measured by observing how far mercury column move along a capillary glass, Twomey[1]. The application of the remote sensing (RS) observations considered here is to analyze the medium properties from a set of radiation intensity measurements, while in a direct solution of the RTE (Radiation Transfer Equation), the medium and the boundary coditions are used to obtain the radiation intensity. Thus the theoretical analysis of the RS method includes the solution of an inverse radiation problem.

Earlier the investigators have considered inverse radiation problems where isotropic radiation is incident on plane parallel, homogenous, isotropically scattering, cf. Siewert[2], as well as anisotrpically scattering media, cf. Kamiuto[3]. Invesigators such as Dunn[4], Ho and Özisik[5] have considered inhomogenities in the medium. Inverse problems other than simple one dimensional systems have not received much attention in the past and only a few studies have appeared in the literature, Kanal and Davies[6], Larsen[7]. The main reasons for this are: (a) there is a lack of efficient direct solution method for multidimensional, inhomogenous, and an isotropically scattering media, which yield accurate radiative intesity distributions and can be employed in iterative or least square minimization based inversion schemes, (b) it is very difficult to develop inverse solution algorithms for general geometries which do not require the solution of the direct problem. Imaging methods such as computed tomography, take advantage of the fact that the medium is thin enough that only the attenuation of uncollided beams of photons are needed to be measured. Then it is possible to estimate the medium composition. The extensive work on inverese analysis of conduction problems by Beck et al.[8] has laid the groundwork for many solution techniques that can be applied to

more general inverese problems. Recent publications have further explored techniques for solving inverse problems that arise in property measurements, remote sensing, structural dynamics, and conduction heat transfer. Diagnostics of hot gases, plumes from high resolution infrared absorption spectroscopy data by using inverse radiative analysis, have become suitable since the development of tunable diode lasers. Thus in non accessible flows of semi-transparent media, which are generally spatially non-homogenous, the reconstruction of their internal compositional structure is nowdays possible by non invasive techniques, Yousefian & Lallemand[9]. The main objective of the work described in this paper is to develop a theoretical model for the interpretation of remote sensing (RS) measurements of pollutants emissions by motor vehicles (The RS method is described in Appendix A), and to extend it to enable measurements of particle concentration. The model is composed of three stages. In the first, the Optical Thickness Equation (OTE) is derived. It is based on the solutions of gaseous diffusion equation and General Dynamic Equation (GDE). The OTE is then applied in order to find gaseous pollutants volumetric flow rates and particles emission rates. In the third stage the mole fractions of CO_2, CO and NO are calculated. The new theoretical model may be applied in the current RS technologies and systems as a supplement tool for monitoring Particulte Matter (PM) emissions. An algorithm has been developed to predict the OT of the medium containing an exhaust gas mixture with scattering soot particles. The particle absorption and scattering efficencies in the UV and IR spectra are calculated according to Mie and Rayleigh theories respectively. The absorption coefficient of the exhaust gas mixture in IR is calculated by the LBL (Line By Line) method. The use of this method for the OT calculations is also new. It is assumed that that the mole fraction of each component in the plume can be calculated according to the Gaussian dispersion model. A new analytical solution for the GDE (General Dynamic Equation) is employed in this algorithm. The calculated results for OT were fitted to the RS measurements results in order to get the gaseous pollutants (NO, HC, CO and CO_2) mole fractions and particles emissions rates in the tailpipe outlet. The new OTE provides an advanced tool for further studies of pollutants spatial distribution and IR and UV radiation attenuation inside the exhaust plume. The results show that the OT increases with the CO_2 and NO mole fractions. The formulation of the OTE is described in section II, and the development of inverse radiative method for the calculation of pollutants concentrations in the tailpipe outlet is described in section VIII.

II. Formulation of the optical thickness equation

The remote sensing (RS) source radiates infra-red rays for the detection of CO_2, CO and an ultra-violet ray for the detection of NO and HC (see Figure 1). The IR and UV radiation absorption of CO, CO_2 and NO in the exhaust plume is determined by using separate band pass filters in the detector, centered at 1.6, 1.565, and 0.226 μm, respectively. According to Shiffelet[10], the UV radiation absorption of HC in the exhaust plume is determined by using band pass filter in the detector, centered between 0.217 μm and 0.223 μm. During the passage of the rays in the plume, the gas molecules and the particles absorb and disperse parts of the radiation. The radiation attenuation depends on the particle size distribution, N, and the gaseous pollutants mole fractions inside the plume, χ_j, with the spectral scattering and absorption coefficients.

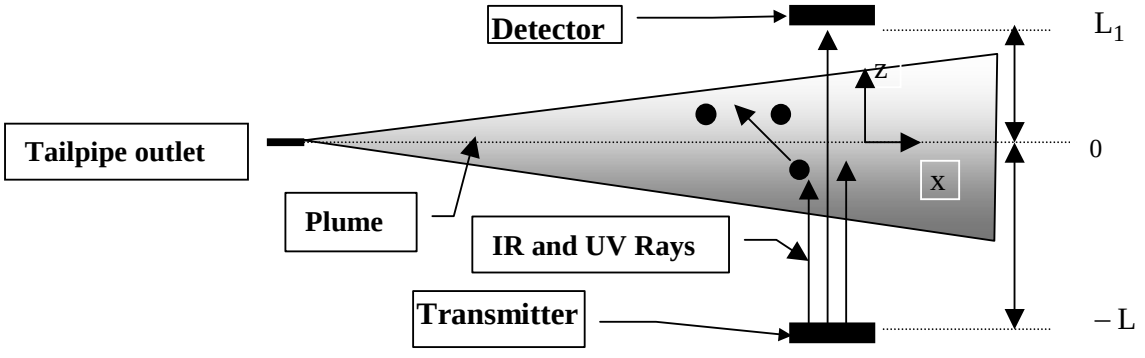

Figure1: Interactions of the radiated rays in the centeral plane (y=0) of the plume.

The OT (optical thickness) of the medium is obtained by integrating the attenuation coefficient between two points -L and L_1:

$$OT = \int_{-L}^{L_1} k_t(s,\nu)ds \qquad (1)$$

where the attenuation coefficient is composed from the absorption and scattering coefficients of the mixture (particles and gas). New expressions for these quantities are derived in the following section for the IR and UV spectra.

III. Radiative properties of particles and gaseous pollutants

Scattering is an encounter between a photon and one or more particles, during which the photon does not lose its entire energy. It may undergo a change in direction and a loss or gain of energy. Scattering can be characterized by four types of events, Siegel and Howell[10]: elastic scattering, in which the energy (and, therefore, frequency and wavelength) of the photon is unchanged; inelastic, in which the energy is changed; isotropic, in which scattering into any direction is equally likely; and anisotropic scattering, in which there is a distribution of scattering directions. Most scattering of importance in engineering is essentially elastic, and the analysis here will consider only this case. For a process with elastic scattering and without emission or absorption, there is no exchange of energy between the radiation field and the medium. Therefore, the thermodynamic conditions of the medium are not affected by the radiation field.

The particles scattering and absorption efficiencies, Q_s and Q_a are defined by:

$$Q_s = \frac{\sigma_s}{\pi r^2} \ , \ Q_a = \frac{\sigma_a}{\pi r^2} \qquad (2)$$

where σ_s and σ_a are the scattering and absorption cross sections, respectively. The efficencies are calculated according to Mie or Rayleigh theories. For particles with radius much smaller than the wavelength, $2\pi r/\lambda <\sim 0.6/n$ (n is the refractive index), the local electric field produced by the wave is approximately uniform at any instant. This applied field induces a dipole in the particle, which oscillates since the electric field oscillates. According to classical theory, it radiates in all directions. This type of scattering is called Rayleigh scattering. A scattering efficiency is derived from quantum or electromagnetic theories. The important result is that for Rayleigh scattering, the scattered energy in any direction is proportional to the inverse fourth power of the wavelength of the incident radiation. The Rayleigh scattering efficiency for unpolarized incident radiation is, Siegel & Howell [11]:

$$Q_s = \frac{8}{3}\xi^4\left(\frac{n^2-1}{n^2+2}\right)^2 \quad ; \quad n = \frac{n_1}{n_2} \qquad (3)$$

Where n_1 and n_2 are the refractive indices of the particle material and the medium respectively. ξ is the size parameter, $\xi = 2\pi r/\lambda$. The Rayleigh absorption efficiency, Q_a, for unpolarized incident radiation is, Siegel & Howell[11]:

$$Q_a = 24\xi\frac{n\kappa}{\left(n^2-\kappa^2+2\right)+4n^2\kappa^2} \quad ; \quad \kappa = \frac{\kappa_1}{n_2} \qquad (4)$$

where κ_1 is the extinction coefficient of the particle. When the scattering particles are not large and are not small enough to fall into the range that is adequately described by Rayleigh scattering, recourse must be taken to more complicated treatments. This is required for the approximate range $0.3 < \xi < 5$. Gustav Mie originally applied electromagnetic theory to derive properties of the electromagnetic field when a plane spectral wave is incident upon a spherical surface, across which the optical properties n and κ change abruptly. The Mie scattering efficiency, Q_s, for unpolarized incident radiation is, Siegel & Howell[11]:

$$Q_s = \frac{8}{3z_A^2}\xi^4\left\{\left[\left(n^2+\kappa^2\right)^2+n^2+\kappa^2-2\right]^2+36n^2\kappa^2\right\}$$
$$\left\{1+\frac{6}{5z_A}\left[\left(n^2+\kappa^2\right)^2-4\right]\left(\frac{2\pi r}{\lambda}\right)^2-\frac{8n\kappa}{z_A}\left(\frac{2\pi r}{\lambda}\right)^3\right\} \quad (5)$$

The Mie extinction efficiency, Q_t, for unpolarized incident radiation is, Siegel & Howell[11]:

$$Q_t = Q_a + Q_s = \frac{24n\kappa}{z_A}\xi+\left\{\frac{4}{15}+\frac{20}{3z_B}+\frac{4.8}{z_A^2}\left[7\left(n^2+\kappa^2\right)^2+4\left(n^2-\kappa^2-5\right)\right]\right\}$$
$$nk\xi^3+\frac{8}{3z_A^2}\left\{\left[\left(n^2+\kappa^2\right)^2+n^2+\kappa^2-2\right]^2-36n^2\kappa^2\right\}\xi^4 \quad (6)$$

where:

$$z_A = \left(n^2+\kappa^2\right)^2+4\left(n^2-\kappa^2\right)+4 \;\;;\;\; z_B = 4\left(n^2+\kappa^2\right)^2+12\left(n^2-\kappa^2\right)+9 \quad (7)$$

The scattering coefficient for the particles, k_s, is calculated according to the following equation:

$$k_s = \int_0^\infty \pi r^2 \cdot N(x,y,z,r)Q_s(r)dr \quad (8)$$

The expression for the particle size distribution, $N(x,y,z,r)$, was obtained in Davidy[12]:

$$N(x,y,z,r) = \frac{Q_p}{4\pi x D^p}\exp\left[-\left(\frac{y^2+z^2}{D^p}\right)\frac{U_v}{4x}\right]\cdot\frac{b^4}{\Gamma(4)}r^3e^{-br} \quad (9)$$

where Q_p is the particle emission rate and D^p is the particle diffusion coefficient. Its value is obtained in Davidy [12]. b is defined as: $b \equiv 3/r_m$, where r_m is the most probable particle radius. Expressions for scattering coefficients over IR and UV spectra are obtained after substitution of Eqs. (3) and (9) into Eq. (8):

$$k_s^{IR} = \frac{Q_p}{4xD^p}\exp\left[-\left(\frac{y^2+z^2}{D^p}\right)\frac{U_v}{4x}\right]\cdot\frac{128\pi^5b^4}{3\lambda^4\Gamma(4)}\left(\frac{n^2-1}{n^2+2}\right)^2\int_0^\infty r^9e^{-br}dr =$$
$$= \frac{128\pi^5Q_p}{12xD^p\lambda^4}\exp\left[-\left(\frac{y^2+z^2}{D^p}\right)\frac{U_v}{4x}\right]\left(\frac{n^2-1}{n^2+2}\right)^2\frac{b^4}{\Gamma(4)}\frac{\Gamma(10)}{b^{10}} \quad (10)$$

In a similar manner, the expression for the Mie scattering coefficient is derived by substitution of Eqs. (5) and (9) into Eq. (8):

$$k_s^{UV} = \frac{Q_p}{4xD^p}\exp\left[-\left(\frac{y^2+z^2}{D^p}\right)\frac{U_v}{4x}\right]\cdot\frac{b^4}{\Gamma(4)}^2\frac{8z_C}{3z_A^2}$$
$$\left\{\left(\frac{2\pi}{\lambda}\right)^4\frac{\Gamma(10)}{b^{10}}+\frac{6}{5z_A}\left[\left(n^2+\kappa^2\right)^2-4\right]\left(\frac{2\pi}{\lambda}\right)^6\frac{\Gamma(12)}{b^{12}}-\frac{8n\kappa}{z_A}\left(\frac{2\pi}{\lambda}\right)^7\frac{\Gamma(13)}{b^{13}}\right\} \quad (11)$$

where

$$z_C \equiv \left[\left(n^2+\kappa^2\right)^2+n^2-\kappa^2-2\right]^2+36n^2\kappa^2$$

The absorption coefficient, k_a, is composed of the particles absorption and gas absorption coefficients:

$$k_a = \int_0^\infty \pi r^2 N(x,y,z,r) Q_a(r) dr + \sum_{j=1}^{N_g} \chi_j k_{a,j} \tag{12}$$

χ_j is the molar fraction of the j component, and N_g is the number of components. This term is calculated by, Wark et al.[13]:

$$\chi_j = \frac{Q_j}{2\pi U_v \sigma_y \sigma_z} \exp\left[-\frac{1}{2}\left(\frac{y^2}{\sigma_y^2} + \frac{z^2}{\sigma_z^2} \right) \right] \tag{13}$$

where σ_y, σ_z are parameters which influence the gas pollutants dispersion inside the plume. They are functions of the downwind position, x, as well as of the atmospheric stability conditions, Wark et al.[13]. These parameters are considered as equal for all the components in the mixture, Mamman[14]. In the model of Chock[15], only three categories of stability criteria were employed to represent microscale atmospheric conditions: stable, unstable, and neutral. Since the RS measurement is carried out in stable conditions, Chok[15]:

$$\sigma_y = \sigma_z = (1.49 + 0.15x)^{0.77} \tag{14}$$

$k_{a,j}$ in Eq. (12) is the absorption coefficient of component j in the IR spectrum. It is calculated by the Line By Line method (LBL). The principles of this method are described in the following section.

An expression for the absorption coefficient in the IR spectrum is obtained by subtitution of Eqs. (9), (13) and (4) into Eq. (12):

$$\begin{aligned} k_a^{IR} &= \frac{Q_p}{4\pi x D^p} \exp\left[-\left(\frac{y^2+z^2}{D^p} \right) \frac{U_v}{4x} \right] \cdot \frac{48\pi^2 b^4}{\lambda \Gamma(4)} f_1(n,\kappa) \int_0^\infty r^6 e^{-br} dr + \sum_{j=1}^{N_g} \chi_j k_{a,j} \\ &= \frac{12\pi Q_p}{x D^p \lambda} \exp\left[-\left(\frac{y^2+z^2}{D^p} \right) \frac{U_v}{4x} \right] f_1(n,\kappa) \frac{\Gamma(7)}{b^7} \frac{b^4}{\Gamma(4)} \\ &+ \sum_{j=1}^{N_g} \frac{Q_j k_{a,j}}{2\pi U_v \sigma_y \sigma_z} \exp\left[-\frac{1}{2}\left(\frac{y^2}{\sigma_y^2} + \frac{z^2}{\sigma_z^2} \right) \right] \end{aligned} \tag{15}$$

where $f_1(n,\kappa)$ is defined by:

$$f_1(n,\kappa) \equiv \frac{n\kappa}{\left(n^2 - \kappa^2 + 2\right)^2 + 4n^2\kappa^2} \tag{16}$$

The expression for the extinction coefficient in the UV spectrum is given by:

$$k_t^{UV} = \int_0^{\infty} \pi r^2 N(x,y,z,r) Q_t(r) dr + \sum_{j=1}^{n} \chi_j k_{a,j} =$$

$$\frac{Q_p}{4xD^p} \exp\left[-\left(\frac{y^2+z^2}{D^p} \right) \frac{U_v}{4x} \right] \cdot \frac{b^4}{\Gamma(4)} \int_0^{\infty} r^5 \left[\frac{24n\kappa}{z_A} \xi + z_D \xi^3 + z_E \xi^4 \right] e^{-br} dr$$

$$+ \sum_{j=1}^{N_g} \chi_j k_{a,j} = \qquad (17)$$

$$\frac{Q_p}{4xD^p} \exp\left[-\left(\frac{y^2+z^2}{D^p} \right) \frac{U_v}{4x} \right] \cdot \frac{b^4}{\Gamma(4)} \left[\frac{24n\kappa}{z_A} \left(\frac{2\pi}{\lambda} \right) \frac{\Gamma(7)}{b^7} + z_D \left(\frac{2\pi}{\lambda} \right)^3 \frac{\Gamma(9)}{b^9} + z_E \left(\frac{2\pi}{\lambda} \right)^4 \frac{\Gamma(10)}{b^{10}} \right]$$

$$+ \sum_{j=1}^{N_g} \frac{Q_j k_{a,j}}{2\pi U_v \sigma_y \sigma_z} \exp\left[-\frac{1}{2} \left(\frac{y^2}{\sigma_y^2} + \frac{z^2}{\sigma_z^2} \right) \right]$$

where

$$z_D \equiv \left\{ \frac{4}{15} + \frac{20}{3z_B} + \frac{4.8}{z_A^2} \left[7\left(n^2+\kappa^2\right)^2 + 4\left(n^2-\kappa^2-5\right) \right] \right\} n\kappa$$

$$z_E \equiv \frac{8}{3z_A^2} \left\{ \left[\left(n^2+\kappa^2\right)^2 + n^2 - \kappa^2 - 2 \right]^2 - 36n^2\kappa^2 \right\}$$

The absorption coefficient is calculated according to:

$$k_a^{UV} = k_t^{UV} - k_s^{UV} \qquad (18)$$

In order to calculate the two radiative properties, k_s and k_a, it is necessary to evaluate the scattering and absorption efficiencies, Q_s and Q_a. For this, the indices of refraction, n, and extinction, κ, of the particles are needed in the IR and UV spectra. Shettle & Fenn[16] obtained some numerical values for these properties for atmospheric soot in the IR spectrum. The results are shown in Figure 2a. Figure 2b illustrates the values of n and κ obtained by Lee & Tien[17] for soot particles in UV spectrum. According to Figure 2a the values of the particles radiative properties at 1.6 μm are: n = 1.77 and $\kappa = 0.465$. According to Figure 2b the values of the particles radiative properties at 0.226 μm are: n = 1.14 and $\kappa = 1.173$.

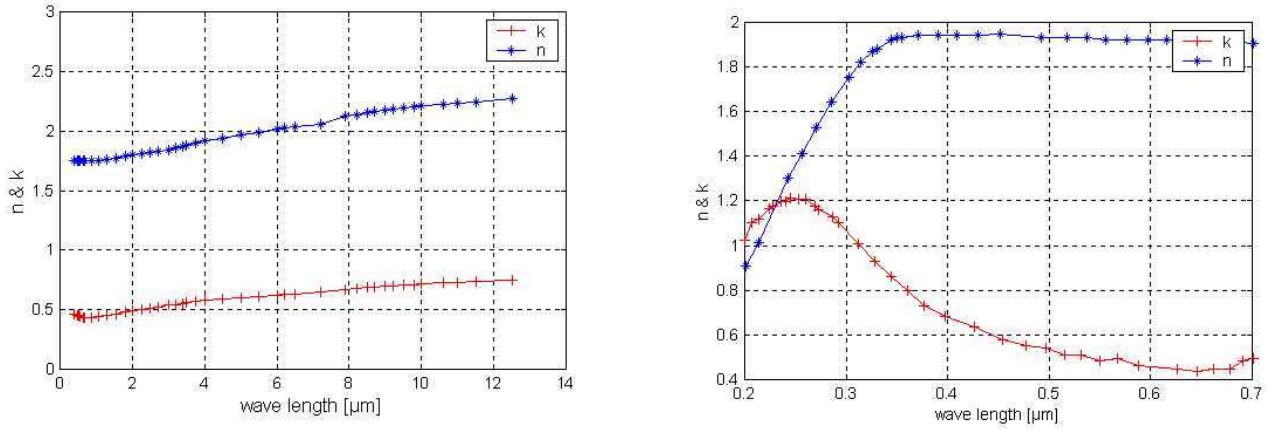

(a) (b)

Figure 2: (a) Dependence of the refractive index, n, and extinction coefficient, κ, on the wavelength, for soot particles in the spectral range 0.4 - 12.5 µm. (b)**:** Dependence of the refractive index, n, and extinction coefficient, κ, on the wavelength, for soot particles in the spectral range 0.2 - 0.7 µm.

IV. IR radiative properties of CO and CO_2 : LBL model

Infrared radiation absorption by CO, CO_2 and H_2O mixtures was calculated here by the Line-By-Line (LBL) method in the wavelength interval of 1.57 - 1.6 µm. This method is the most accurate one for radiative transfer in hot gases and for the determination of gas radiation properties. It is used as a reference model for validating other (approximate) models. The LBL approach takes into account, at high resolution, the contributions of all the significant absorbing lines of the various species in the mixture, cf. Taine et al.[18]. A line i, centered at wave number ν_i, is characterized by an intensity $S_i'(T_S)$, at the standard temperature $T_S = 298\,K$, and a normalized profile $F_i(\nu - \nu_i)$, of the Lorentz, Voigt or Doppler type. The absorption coefficient for the component j, $\kappa_{\nu,i}^j$, at wave number ν, associated with line i, is:

$$\kappa_{\nu,i}^j = n_j S_i'(T) F_i(\nu - \nu_i) \tag{19}$$

where n_j is the number of absorbing molecules per unit volume. The line intensity at a given temperature T is given by:

$$S_i'(T) = S_i'(T_S)\exp\left[-\frac{E''}{k_B}\left(\frac{1}{T}-\frac{1}{T_S}\right)\right] * \frac{Q(T)}{Q(T_S)}\frac{1-\exp\left(-\frac{hc\nu_i}{k_B T}\right)}{1-\exp\left(-\frac{hc\nu}{k_B T}\right)} \tag{20}$$

where E'' is the energy of the lowest quantum level of the transition associated with the line, $Q(T)$ is the partition function of the absorbing molecule, h and k_B are the Planck and Boltzmann constants, and c is the speed of light in the medium. The total absorption coefficient for j is calculated according to:

$$\kappa_\nu^j = \sum_{i=1}^{\infty} \kappa_{\nu,i}^j \tag{21}$$

Combined Natural, Collision, and Doppler Profiles

The rest-frame line profile of a radiating (or absorbing) species is most often Lorentzian (natural or collisional). However, there is also relative motion between the emitter and the observer or between the source and the absorber, resulting from the thermal energy of the atoms (or molecules). The thermal motion (assumed Maxwellian) of the radiating species leads to a Gaussian line profile. Clearly, in most situations of interest, the actual line profile involves a convolution of these two types of broadening mechanisms. Thus the actual profile function can be written in the form of the convolution, cf. Measures[19]:

$$F_i(\nu - \nu_i) = \int_{-\infty}^{\infty} G(\nu_i) D(\nu, \nu_i) d\nu_i \qquad (22)$$

where $D(\nu, \nu_i)$ is the Lorentzian probability of absorption at ν for an absorber having a line with wave number ν_i. $G(\nu_i)d\nu_i$ is the Gaussian probability of an absorber having a line in the interval $(\nu_i, \nu_i + d\nu_i)$, due to its thermal motion. The LBL calculation is based on the HITRAN database, Rothman et al.[20].

V. LBL Model Results and Discussions

The LBL method has been employed to calculate the absorption spectra of the exhaust gas components CO, CO_2 and H_2O at the wavelengths 1.57 and 1.6 μm. Figure 3a shows the calculated absorption spectra of gas columns with pure CO_2 and pure CO in the wavelength interval 1.56 - 1.8 μm. As can be seen, the absorption coefficient of CO_2 is practically zero in this interval below 1.565 μm, and then at the larger wavelengths, it increases to the same order of that for CO. It can also be seen that the absorption coefficient of CO_2 is higher than that of CO at wavelengths larger than 1.6 μm. In order to understand what is the contribution of the H_2O absorption coefficient to the overall gaeous absorption coefficient in these intervals, the absorption spectra of H_2O was calculated, and the results are presented in Figure 3b for the intervals 1.56 - 1.62 μm. As can be seen, the H_2O absorption coefficient is negligible compared with those of CO or CO_2: less than 1% in both intervals. According to Figure 3a, the absorption coefficient of CO_2 is 0.065 1/m at 1.603 μm.

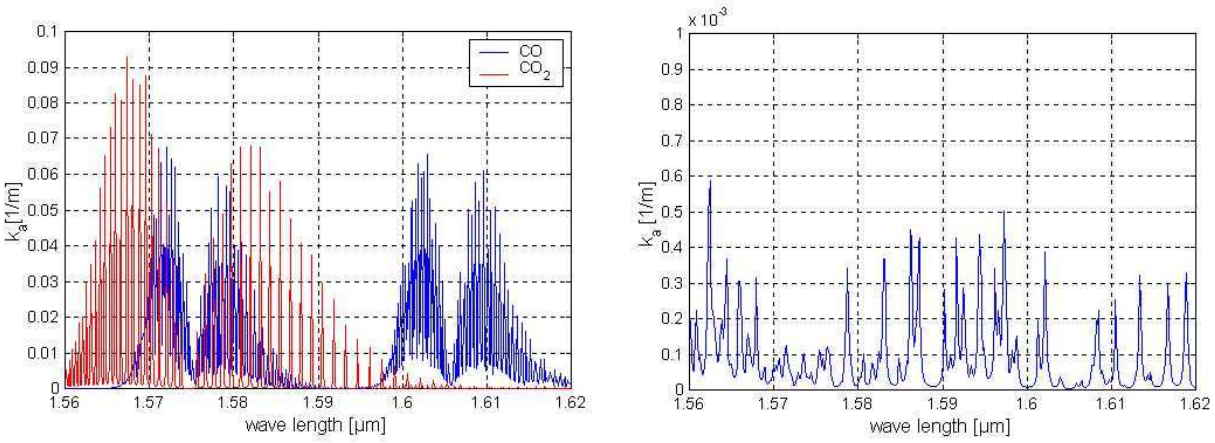

(a) (b)

Figure 3: LBL calculations of absorption spectra for gas columns at temperature 313 K and pressure 1 bar: (a) pure CO_2 and CO. (b) pure H_2O.

VI. UV radiative properties of NO

According to Chan et al.[21], the absorption cross-section of NO at 0.226 μm (5.47 eV) is $\sigma_{a,NO} = 0.555$ Mbarn (1barn = 10e-24 cm²). The absorption coefficient of NO is calculated according to:

$$k_a^{NO} = n_{NO}\sigma_{a,NO} \tag{23}$$

where n_{NO} is the number of NO molecules per unit volume, derived by using the equation of state of ideal gas, Dalton rule and Eq. (13):

$$n_{NO} = \frac{\chi_{NO}p}{\overline{R}T}Na = \frac{pNa}{\overline{R}T}\frac{Q_{NO}}{2\pi U_v\sigma_y\sigma_z}\exp\left[-\frac{1}{2}\left(\frac{y^2}{\sigma_y^2}+\frac{z^2}{\sigma_z^2}\right)\right] \tag{24}$$

VII. Derivation of the optical thickness equation for IR and UV spectra

The expressions for the integral of the attenuation coefficient over the distance are obtained by introducing Eqs. (10) and (15) into Eq. (1) for the IR spectrum and Eq. (17) into Eq. (1) for the UV spectrum.

$$\begin{aligned}
OT_i^{IR} &= \left[\int_{-L}^{L_1} k_t dz\right]_{IR} = \left[\int_{-L}^{L_1}(k_s+k_a)dz\right]_{IR} = \left\{\frac{12\pi Q_p}{xD^p\lambda}f_1(n,\kappa)\frac{b^{-3}\Gamma(7)}{\Gamma(4)}\right. \\
&\left.+\frac{128\pi^5 Q_p}{12xD^p\lambda^4}\left(\frac{n^2-1}{n^2+2}\right)^2\frac{b^{-6}\Gamma(10)}{\Gamma(4)}\right\} \\
&\left[\operatorname{erf}\left(L\sqrt{\frac{U_v}{4D^p x}}\right)+\operatorname{erf}\left(L_1\sqrt{\frac{U_v}{4D^p x}}\right)\right]\exp\left[-\frac{y^2}{D^p}\frac{U_v}{4x}\right]\sqrt{\frac{\pi D^p x}{U_v}} \\
&+\sum_{j=1}^{n}\frac{Q_j k_{a,j}}{2\pi U_v\sigma_y\sigma_z}\exp\left[-\frac{y^2}{2\sigma_y^2}\right]\frac{\sqrt{2\pi}\sigma_z}{2}\left[\operatorname{erf}\left(\frac{L}{\sqrt{2}\sigma_Z}\right)+\operatorname{erf}\left(\frac{L_1}{\sqrt{2}\sigma_Z}\right)\right]
\end{aligned} \tag{25}$$

$$\begin{aligned}
OT_i^{UV} &= \left[\int_{-L}^{L_1} k_t dz\right]_{UV} = \frac{Q_p}{4xD^p}\exp\left[-\frac{y^2}{D^p}\frac{U_v}{4x}\right]\cdot\frac{b^4}{\Gamma(4)} \\
&\left[\frac{24n\kappa}{z_A}\left(\frac{2\pi}{\lambda}\right)\frac{\Gamma(7)}{b^7}+z_D\left(\frac{2\pi}{\lambda}\right)^3\frac{\Gamma(9)}{b^9}+z_E\left(\frac{2\pi}{\lambda}\right)^4\frac{\Gamma(10)}{b^{10}}\right] \\
&\frac{\sqrt{\pi D^p x}}{\sqrt{U_v}}\left[\operatorname{erf}\left(\frac{L\sqrt{U_v}}{\sqrt{4D^p x}}\right)+\operatorname{erf}\left(\frac{L_1\sqrt{U_v}}{\sqrt{4D^p x}}\right)\right] \\
&+\sum_{j=1}^{n}\frac{Q_j k_{a,j}}{2\pi U_v\sigma_y\sigma_z}\exp\left[-\frac{y^2}{2\sigma_y^2}\right]\frac{\sqrt{2\pi}\sigma_z}{2}\left[\operatorname{erf}\left(\frac{L}{\sqrt{2}\sigma_Z}\right)+\operatorname{erf}\left(\frac{L_1}{\sqrt{2}\sigma_Z}\right)\right]
\end{aligned} \tag{26}$$

It can be seen from Eqs. (25) and (26) that the OT is composed of two terms. The first represents the scattering and absorption of the IR and UV radiation by the particles. The second represents the radiation absorption by the exhaust gas components. The RS measurements output files already contain the values of the optical thickness in each wave length: 0.217 to 0.223μm, 0.226 μm,1.565 μm and 1.6μm, Shiffelet[10].

VIII. Development of inverse radiative method for the calculation of pollutants concentrations in the tailpipe outlet

The retrieval of the gaseous pollutants concentrations and particles emission rates in the tailpipe outlet is described in this section. The input data required for the calculation of these parameters are: the ambient temperature, T, the

vehicle velocity, U_v, and the road width, $L+L_1$. At first, the volumetric flow rates of the gaseous pollutants (Q_{NO}, Q_{CO} and Q_{CO2}) and the particles emission rate, Q_p in the tailpipe outlet, are calculated by fitting the theoretical results for the OT (see Eqs. (25) and (26)) to the measured OT. Then the NO, CO and CO_2 mole fractions $(y_{NO}, y_{CO}, y_{CO_2})$ are calculated by using the Amagat relations (ideal gas mixture), i.e:

$$y_{CO}/y_{CO2} = Q_{CO}/Q_{CO2} \tag{27}$$

$$y_{NO}/y_{CO2} = Q_{NO}/Q_{CO2} \tag{28}$$

Bishop & Stedman[22] derived an empirical equation between the CO and CO_2 mole fractions based on the chemical combustion equation:

$$y_{CO} + 1.3963 y_{CO2} = 0.2101 \tag{29}$$

Eq. (27) is introduced into Eq. (29), in order to obtain the CO and CO_2 mole fractions in the tailpipe outlet.

$$y_{CO} = \frac{0.2101 Q_{CO}/Q_{CO2}}{1.3963 + Q_{CO}/Q_{CO2}}$$
$$y_{CO_2} = \frac{0.2101}{1.3963 + Q_{CO}/Q_{CO2}} \tag{30}$$

The seven parameters $y_{NO}, y_{CO}, y_{CO_2}, Q_{NO}, Q_{CO}, Q_{CO_2}$ and Q_p are calculated by the equations, (25 – twice, for the pairs Q_{CO}, Q_p and Q_{CO_2}, Q_p), (26 - for Q_{NO}), (27), (28), (29) and the curve fitting of the theoretical and measured OT. It can be seen from Eqs. (28) and (30) that the derived gaseous pollutants mole fractions at the tail pipe outlet depend only on the ratios of the CO and NO volumetric flow rates to that of the CO_2. It is estimated that the errors involved in the calculations are small, since the model compensates for errors resulting from different effects, such as: the location of the exhaust gas plume with respect to the beam, the fluctuations in the transmitted radiation signals, the total emission rate from the vehicle engine, etc, cf. Bishop and Stedman[22]. The theory on which the operation of the current RS method is based was explained in Davidy[12].

IX. Model Results and Discussion

Theoretical and measured results are presented here for the gaseous pollutants concentrations. RS experiments were carried out during the summer 2001, where emissions of about 14,000 vehicles were measured. Some examples are presented in this paper. The example, which is described here, was monitored on 9/8/2001 (sequence no. 387). The measured wind and vehicle speeds were 4.5 and 46.9 km/h respectively. Figure 4 shows a comparison between the fitted and the measured values of OT_{CO}. As can be seen, the agreement is quite good. Table 1 shows a comparison between measured and calculated values of pollutants concentrations. It can be seen that the calculated result for the CO mole fraction is a little lower than the measured value. This is because the absorption coefficient of this component is low (see Figure 3a). Thus the IR radiation is absorbed and scattered mostly by the particles. Therefore, the correlation between the theoretical and measured results is not very good (see Eq. (25)). The difference between the calculated and measured NO mole fractions can be explained based on the fact that the calibration during the NO measurement was not accurate (at that time, NO and CO_2 calibration gaseous mixture was not available).

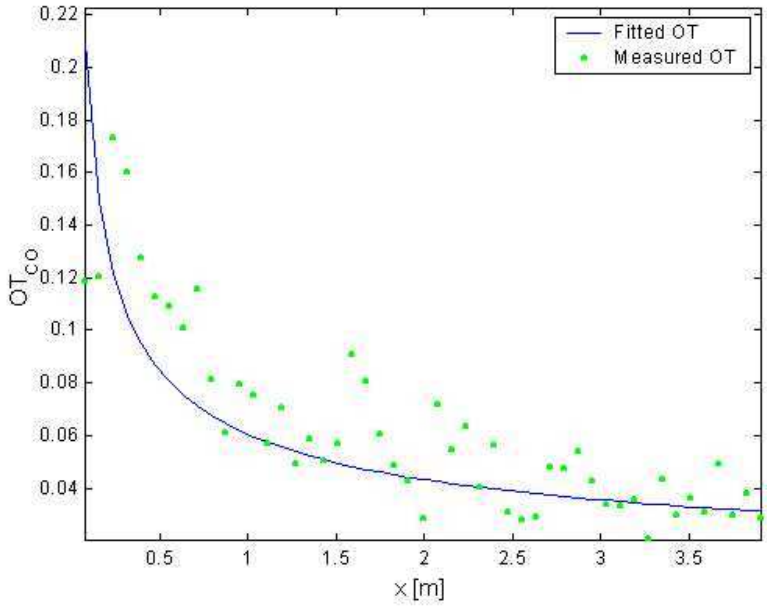

Figure 4: Comparison between the calculated and measured values of the OT_{CO} (sequence 387).

Table 1: Comparison between calculated and RS measured emission results (monitored on 9/8/2001 sequence 387).

Pollutant	Q_i	y_i Calculated according to the Bishop & Stedman equation	by y_i Measured RS system
CO2	$0.015\,m^3/s$	8.77 %	9.91 %
CO	$0.015\,m^3/s$	8.77 %	7.77 %
NO	$10^{-7}\ m^3/s$	58.46 ppm	353 ppm
PM	$2.5\cdot10^8\ 1/s$	------	------

X. Summary and Conclusions

This paper includes a presentation of a new theoretical model for the interpretation of remote sensing measurements of gaseous pollutants and particulates emissions by motor vehicles. This model is based on the solutions of Optical Thickness Equation (OTE), gaseous diffusion equation and General Dynamic Equation (GDE) for the particles. An algorithm has been developed to predict the attenuation coefficient of the medium containing an exhaust gas mixture with scattering and absorbing soot particles. The solution of the OTE gives the gaseous pollutants (NO, CO and CO_2) concentrations and particles emissions rates in the tailpipe outlet. The absorption and scattering efficiencies of the particles were calculated according to Mie or Rayleigh theories, and the absorption coefficients by the Line-by-Line (LBL) method. Analytical solutions to the GDE were obtained for particles number concentrations. Theoretical and measured results are presented here for the gaseous pollutants concentrations. RS experiments were carried out during the summer 2001, where emissions of about 14,000 vehicles were measured. Numerical results (for optical thickness) of the present model compare favorably with the experimental data. It was shown that the theoretical results are similar to the measured results for large CO concentrations, when the IR radiation (at 1.565μm wavelength) absorption is strong.

Appendix A: Measurements of Vehicle emissions by Remote Sensing

The remote sensing method for measuring pollutants concentrations is based on the attenuation of electro-magnetic (or laser) beams, which are radiated from a source, traverse through the exhaust gas plume and detected by a sensor. A schematic arrangement of the system for measuring emissions from vehicles (while driving) appears in Figure A.1.

The source emits infra-red rays for the detection of CO_2, CO and an ultra-violet rays for the detection of HC and NO.

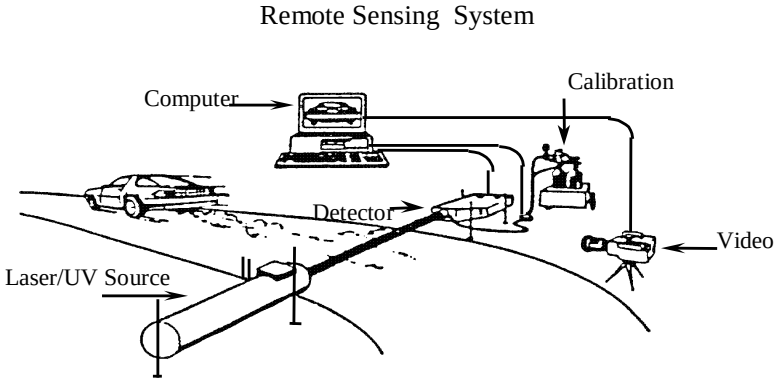

Figure A.1: Schematic of remote sensing system for measurements of vehicle emissions.

During the passage of the rays in the plume, the gas molecules and the particulates absorb and disperse parts of the radiation. Thus the energy reaching the sensor is lower than that leaving the source. The attenuation of the intensity depends on the pollutants concentrations, and the system computer performs the calculations and displays them on the monitor. A video camera records the license plate of the vehicle, in order to obtain, later, its specifications (mainly manufacturer, age and engine displacement). The system measures the car speed and acceleration, which also appear on the monitor.

Theory of RS operation

The RS operation theory is based on NDIR (NDUV for NO). The TDL (Tunable Diode Laser) technology is used to monitor the emissions in the IR spectrum and Deuterium lamp in the UV spectrum. TDLs are small crystals of Ga, As, Sb and P. Each TDL emits a laser beam at a specific wavelength when an electric current is applied (see Figure A.2). The radiation wavelength is determined by the composition of the crystal. It can also be changed over a narrow range by varying the current applied to the crystal, thus allowing scanning across an absorption line. Since the wavelengths emitted are very precise, an interference-free absorption band for each component of interest is selected for the analysis.

CO and CO_2 are measured by making use of IR absorption in the wavelength range near 1.6 μm. HC and NO are measured in the UV (ultraviolet) absorption, in the wave length range 0.217 to 0.223 μm and 0.225 to 0.228 μm, respectively, Shiffelet[10]. The use of UV absorption for NO has several advantages, Bishop & Stedman[22], e.g. an absorption coefficient of about 1000 times larger than in the IR spectrum, giving rise to larger signals. Moreover, there is no interference with water vapor in the UV. The atmosphere is optically transparent to UV radiation and many components of hydrocarbons absorb radiation in the UV spectrum. The measurement is based on initial calibration against a gas mixture, which contains CO_2, CO and NO. For HC calibration, use is made of butadiene as a reference gas. During the calibration process, fits are made to plot the mole fractions versus optical thickness. These equations are subsequently used to derive mole fractions from the optical thickness measured inside exhaust plumes. The RS system measures the spectrum of the background signal received from the deuterium lamp and TDL before the car passes, B(λ), and the spectrum of the sample signal received after the car passes, S(λ), Shiffelet[10]. S(λ) is smaller than B(λ) because of the radiation attenuation in the exhaust plume. The OT (Optical Thickness) is calculated according to the Beer (Lambert) law:

$$\mathrm{OT}_m(\lambda) = -\ln\left(S(\lambda)/B(\lambda)\right) \qquad (A.1)$$

Each sample mole fraction is calculated by using a linear square fitting procedure, placing the reference optical thickness, OT_r, which was obtained in the laboratory, with a known mole fraction of the reference gas over a known path-length on the x axis and OT_m on the y axis.

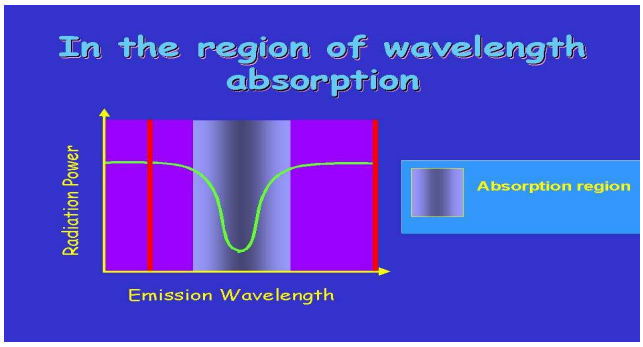

Figure A.2: Results of a scan across an absorption band for exhaust component.

The resulting slope (e.g. by least square fitting between the measured and references optical thicknesses) is proportional to the sample mole fraction in the beam path. This procedure corrects the CO, HC, CO_2 and NO signals, that could occur due to source intensity and signal strengths fluctuations, that would result from the presence of particulate matter (e.g., from either the vehicle exhaust or from the roadway) between source and detector, Stephens & Cadle[24]. In the RS equipment used in this work, the above sequence of measurements and calculations is repeated 50 times, at 6 ms intervals, for a total of 300 ms of data.

Because the plume path thickness which is radiated depends on turbulence and wind intensities, one can only determine the ratios of CO, HC and NO to CO_2, Shiffelet[10]. According to the manufacturer of the system, the measurements of ratios of the pollutants concentrations to that of the CO_2 is more accurate since it compensates for errors resulting from such effects as location of the exhaust gas plume with respect to the beam, wind, total emission rate from the vehicle engine, etc. In addition to that, it is assumed that CO, HC, NO and CO_2 within an exhaust plume disperse at an equal rate, which means that although these concentrations vary rapidly with time, the CO/ CO_2, NO/ CO_2 HC/ CO_2 ratios are constant, Stephens & Cadle[24]. In order to provide the dry CO_2 mole fraction, the values of the ratios: Q for CO/CO_2, Q' for HC/CO_2 and Q'' for NO/CO_2 are used in the combustion equation, cf. Bishop & Stedman[22]:

$$y_{CO_2} = \frac{0.42}{2.79 + 2Q + 0.42 \cdot Q' + Q''} \qquad (A.2)$$

The dry CO, HC and NO mole fractions are obtained according the following equations, cf. Bishop & Stedman[22]:

$$y_{CO} = y_{CO_2} Q = \frac{0.42Q}{2.79 + 2Q + 0.42 \cdot Q' + Q''}$$

$$y_{HC} = y_{CO_2} Q' = \frac{0.42Q'}{2.79 + 2Q + 0.42 \cdot Q' + Q''} \qquad (A.3)$$

$$y_{NO} = y_{CO_2} Q'' = \frac{0.42Q'}{2.79 + 2Q + 0.42 \cdot Q' + Q''}$$

These equations are applied to calculate the gaseous pollutants mole fractions in the outlet of the tailpipe from radiation intensities detected in each wavelength.

Acknowledgement

The financial help of the Technion is gratefully acknowledged. The financial support of the Alice Schuster Fund and the General Motors Foundation is greatly appreciated. The authors also thank the MD Lasertech Co., the Israeli Ministries of Environment and of Transportation and the Haifa Municipality for their valuable assistance in carrying out RS and roadside emission measurements and for providing data about the vehicles which were tested. This paper describes part of the Ph.D. work of Alon Davidy, in the Technion, Israel Institute of Technology, Haifa, Israel.

References

[1]Twomey, S., Introduction to the Mathematics of Inversion in Remote Sensing and Indirect Measurements, Developments in Geomathematics 3, Elsevier Scientific Publishing Company, 1979.

[2] Siewert, C.E, A new approach to the inverse problem, *J. Math. Phys.*, Vol. 19, 1978,pp. 2619-2621.

[3]Kamiuto, K., A Constrained Least Squares Method for Limited Inverse Scattering Problems, *J. Quant. Spectrosc. Radiat. Transfer*, Vol. 40, 1988,pp. 47-50.
[4]Dunn, W.L., Inverse Monte Carlo Analysis, *J. Comput. Phys.* 41 (1981) 154-166.
[5]Ho, C.H. & Özisik, M.N., Inverse Radition Problems in Inhomogenous Media, *J. Quant. Spectros. Radiat. Transfer*, Vol. 40, 1988, pp. 553-560.
[6]Kanal, M. & Davies, J.A., A multidimensional inverse problem in Transport Theory, Transport Theory *Statist. Phys*., Vol. 8, 1979, pp. 99-115.
[7]Larsen, E.W., Solution of Three Dimensional Inverse Transport Problems, *Transport Theory Stati. Phys*., Vol. 17 , 1988, pp. 147-167.
[8]Beck, J.V., Alifanov, O.M., Woodbury, K.A., Artyukin, E.A., & MacCormick, N., Joint American-Russian NSF Worksop on Inverse Problems in Heat Transfer, Final Report MSU-ENGR-92-008, Micjigan State University, 1992.
[9]Yousefian , F. & Lalleman, M., Temperature and Species concentration Profiles using High Resolution Infrared Transmission Data by Inverse Radiative Analysis, Radiative Transfer II, Second International Symposium Radiative Heat Transfer, Pinar Menguc, ed. Kusadsi, Turkey, Begell House, New York, 1998, pp. 329-340.
[10]Shiffelet, P. Private communication.
[11]Siegel, R. & Howell, J.R., *Thermal Radiation Heat Transfer*, Hemisphere Publishing Corporation, 4th Edition, 2002.
[12]Davidy, A., *Theoretical and experimental study of remote sensing for measuring emission of pollutants, Ph. D. thesis, Technion*, Israel, 2004.
[13]Wark, K., Warner, C.F. & Wayne T.D., *Air Pollution Its Origin and Control*, Addison Wesley, 1998.
[14]Mammane, Y., private communication.
[15]Chock, D.P., A Simple Line-Source Model for Dispersion Near Roadways, *Atmospheric Environment*, Vol. 12, 1978,pp. 823-829.
[16]Shettle, E.F. & Fenn, R.W., Models of the lower atmosphere and the effects of humidity variations on their optical properties, Air Force Geophysics Laboratory Report AFGL-TR-79-0214, Environmental Research Papers, N0676, 1979.
[17]Lee, S.C. & Tien, C.L., 1981, Optical Constants of Soot in Hydrocarbon Flames, *18th Symposium on Combustion*, The Combustion Institute, 1981, pp.1159-1166.
[18]Taine, J., Soufiani, A., Riviere, P. & Perrin, M.Y., Recent Developments in Modeling the Infrared Radiative Properties of Hot Gases, Proc. of 11th IHTC, August 23-28, 1998, Kyongju, Korea, 1998, pp. 175-187.
[19]Measures, R.M., Laser Remote Sensing Fundamentals and Application, John Wiley & Sons, 1984.
[20]Rothman, L.S., Rinsland, C.P., Goldman, A., Massie, S.T. Edwards, D.P., Flaud, J.M., Perrin, A., Camy-Peyret, C., Dana, V., Mandin, J.Y., Schroeder, J., McCann, A., Gamache, R.R., Wattson, R.B., Yoshino, K., Chance, K.V., Jucks, K.W., Brown, L.R., Nemtchinov, V., and Varanasi, P., The HITRAN Molecular Spectroscopic Database and HAWKS (HITRAN Atmospheric Workstation): 1996 Edition, *Journal of Quantitative Spectroscopic and Radiative Heat Transfer*, Vol. 60, 1998, pp. 665-710.
[21]Chan, W.F., Cooper, G. & Brion, C.E., Absolute Optical Oscillator Strengths for the Photo-absorption of Nitric Oxide (5-30 eV) at high resolution, *Chemical Physics*, Vo. 170, 1993, 111-121.
[22]Bishop, G.A. & Stedman, D.H., Measuring the Emissions of Passing Cars, *Accounts of Chemical Research*, Vol. 29, 1996, pp.489-495.
[23]Stedaman, D.H., Bishop, G. & Maclaren, S., 1996, Apparatus for Remote Analysis of Vehicle Emissions, *US. Patent no. 5,498,872*.
[24]Stephens, R.D. & Cadle, S., Remote Sensing Measurements of Carbon Monoxide Emissions from On-Road Vehicles, *Journal of Air Waste Management*, Vol. 41, 1991, pp. 39-46.